

Hydraulic Analysis with CFD – Flow 3D Numerical Modeling of Local Erosion in Bridge Piles

Khaled Hamad*, Cristina Torres

National Polytechnic School, Ecuador.

*Corresponding author. Email address: khaled.hamad@epn.edu.ec

Abstract: Within the Centro de Investigaciones y Estudios en Recursos Hídricos (CIERHI), the experimental analysis was carried out in a physical model of turbulence phenomena, which causes erosion around bridge piers (Chiliquinga & Pinto, 2019). The data of the experimental model was used as a calibration base for the three-dimensional numerical modeling of erosion around bridge piers, using the FLOW-3D computational package. Once the model was calibrated, the conditions with which the physical model was made were improved, since in the experimental results, it was determined that a deeper sand bed was necessary to be able to determine the maximum erosion. In the numerical model, the optimal conditions were placed to obtain results without the physical limitations that exist in an experimental model, thus obtaining results of maximum local scour in pier bridge, and these results were compared with values calculated based on different empirical equations.

Key words: erosion; piers; simulation; modelling; scour; FLOW-3D

1. Introduction

In the field of hydraulic engineering, river flow and the problems associated with it, such as sediment transport, river bed deformations, scour and flooding, are considered the main problems of a country. Most bridge failures are due to scour and an example of this is the study by the U.S. Federal Highway Administration in 1973, which determined that, of 383 cases of bridge failures observed, 97% were caused by hydraulic problems of local erosion: 25% in piers and 75% in abutments; that is, only 3% of the recorded failures were due to causes unrelated to hydraulics (Fernández, 2004).

Within the Centro de Investigaciones y Estudios en Recursos Hídricos (CIERHI), the experimental analysis was carried out in a physical model of turbulence phenomena, causing erosion around bridge piers (Chiliquinga & Pinto, 2019). In the experimental results, it was determined that a higher sand bed was necessary to determine the maximum erosion depth. In addition, the channel walls of the physical model directly influenced the results, because the friction along the channel walls affects the velocity distribution of the central region. This phenomenon could be avoided if the experimental analysis is carried out in a wide open channel (if the width is greater than 5 to 10 times the flow depth) (Chow, 2004). In the numerical model, the optimal conditions were placed to obtain results without the physical limitations of an experimental model, such as the height of the sediment bed and the width of the channel, which in the physical model was

placed with negligible friction on the walls.

2. Methodology

2.1 Physical model (Experimental analysis in physical model of turbulence phenomena causing erosion around bridge piers using ADV) (Chiliquinga & Pinto, 2019).

Within the Centro de Investigaciones y Estudios en Recursos Hídricos (CIERHI), the turbulence phenomenon that causes erosion and undermining of solid material around a bridge pier was experimentally analyzed (Chiliquinga & Pinto, 2019). The tests were carried out in the CIERHI hydrodynamic channel, a sediment bed 2 m long, 12 cm high was placed, occupying the total width of the channel of one meter. Two concrete piers, both 90 cm high, were used in separate tests. For the first test, a square cross-section pier with a width of 10 cm was used. In the second test, a circular cross-section pier with a diameter of 10 cm was used. The piles were placed 50 cm from the edge of the sediment bed. Figure 1 shows the location of the piles.



Figure 1. Location of the square and circular pile on the sand bed.

The conditions for the movement threshold were determined through experiments, and the threshold or movement principle was calculated using a shield diagram, with the aim of preventing sand from moving without piles and analyzing the erosion of the riverbed around the piles due to the presence of this structure. Experimentally, the start of particle movement occurred at a depth of 0.205 m, using the shields diagram for the calculation of the threshold or principle of movement a depth of 0.21 m was determined, verifying coincident values experimentally and analytically.

The boundary conditions used in the physical model are: flow rate 52.47 l/s, depth 0.25 m which gives a speed of 0.21 m/s.

The sediment used in the physical model has the following properties (Chiliquinga & Pinto, 2019):

Specific weight of the sediment = 2.65 t/m³

$D_{16} = 0.403$ mm; $D_{50} = 0.739$ mm; $D_{84} = 1.072$ mm; $D_{90} = 1.142$ mm

The representative sizes of the sediment are: diameter 0.85 mm with 20.4%, diameter 0.71 mm with 36.7% and 0.6 mm with 36.6%.

According to the classification of sediments (sand) by size, the group and class of sediment corresponds to coarse sand. The calculation of the typical particle size deviation of the material yields a result of 1.63 (Chiliquinga & Pinto, 2019). The typical particle size deviation allows determining the type of particle size of the sample. In this case, a value of less than three is obtained, which indicates that the particle size is uniform, a typical condition in sediments used in the laboratory (synthetic material).

In the physical model without placing the piles, the conditions of the principle of movement were determined experimentally, varying the draft with the help of a gate located downstream of the bed, the flow rate was maintained, and the water height was reduced until the movement of the particles began.

The threshold or principle of particle movement was also calculated using the shields diagram, which is generated when the bed tension and the critical tension are equal. This procedure is carried out to ensure the condition of Aguas Claras (which means that the flow does not reach the critical speed, and by not having enough force to mobilize the particles of the bed, there is no generalized movement, erosion could only occur if an obstacle is found, therefore, the only possible erosion is local). A draft was placed that does not generate the movement of particles without the pile since what is to be evaluated is precisely the erosion that the bed suffers around a pile due to the presence of said structure (Chiliquinga & Pinto, 2019). It was not possible to determine the results of maximum erosion in the physical model because after four hours of testing, the scour around the square and circular pile reached 12 cm of the sand bed.

2.2 Numerical model (calibration)

Computational Fluid Dynamics (CFD) uses specially developed numerical techniques to solve the equations of fluid motion and obtain three-dimensional solutions (FLOW-3D, n.d.).

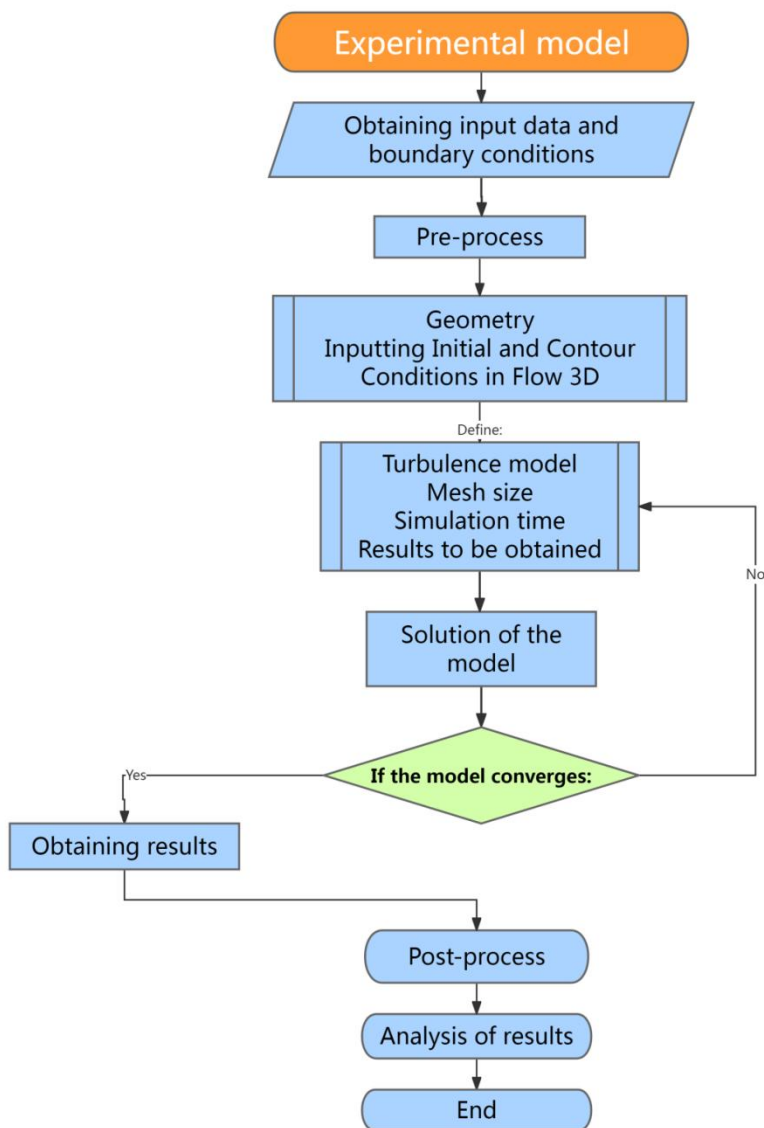


Figure 2. Flow chart of the experimental model.

In this project, the commercial software FLOW-3D was used. It is a three-dimensional (3D) hydraulic modeling program developed in 2000 by Flow Science; it solves the Navier-Stokes equations using numerical approximations (FLOW-3D, n.d.). FLOW-3D is the most widely used commercial software for free-surface flow modeling, generating an accurate simulation of various engineering problems related to water and the environment. In FLOW-3D, it is possible to determine sediment transport processes, for example: bed transport, suspended solids transport, drag and deposition (Weig et al., 2014).

To solve the hydraulic model, we have three stages: preprocessing, which refers to the input data before operation, such as geometry, geometric mesh, physical properties, initial conditions, and boundary conditions; preprocessing refers to the operation of the model, while post-processing is the analysis of the results. For the calibration of the numerical model, the geometry, boundary conditions and sediment properties of the physical model were used.

2.2.1 Geometry

The geometry of the physical model was entered for the calibration of the numerical model of the square and circular pile. The channel bottom was entered as a 10 cm high solid and the piles were placed as a solid with the dimensions of the physical model, while the granular material was entered with the packed sediment option.

2.2.2 Physical mechanisms

Gravity - applies a constant force to the model that refers to the effect of gravity, and the value of - 9.81 was entered in the direction of the Z axis.

Sediment transport - The FLOW-3D software allows the use of a sediment transport model with multiple granular sediment diameters, up to a maximum number of 10 particle sizes in the same bed. Calculates particle movement by (FLOW-3D, n.d.):

- Suspension
- Sedimentation by gravity
- Material drag due to bed shear or flow disturbances
- Bottom sediment transport (rolling, sliding or jumping)

For this, two states are considered: suspended sediment and compacted sediment. Suspended sediment is transported by flow turbulence. Below are the input parameters of the sediment transport model shown by the FLOW-3D software and the parameters selected for calibration and final run within the project: for the simulation, the following physical mechanisms were included in the calculation:

Table 1. Input parameters – sediment transport

Input parameter		Value or equation
a	Shields critical number	Soulsby-Whitehouse
b	Background transport equations	Meyer Peter & Müller
c	Richardson-Zaki multiplication coefficient Suspended sediment diffusion Turbulent diffusion multiplier	1 0 kg/m/s 1.43
d	Maximum compaction fraction	0.64
e	Bed roughness ratio / D50	2.5

Input parameter		Value or equation
f	Types of sediment	0.85mm (20.4%) 0.71mm (36.7%) 0.60mm (36.6%)
	Particle density Drag coefficient Bed loading coefficient Angle of repose	2650 kg/m ³ 0.018 13 25 degrees

a. Shields critical number

The Shields critical number is a dimensionless parameter used to calculate the onset of sediment transport or threshold of the beginning of sediment movement in the flow of a fluid (Shields, 1936). The calculation option using the Soulsby-Whitehouse equation was selected (Soulsby, 1997):

$$\theta_{cr,i} = \frac{0.3}{1+1.2d_i} + 0.055 (1 - e^{-0.02d_i}) \quad (1)$$

Where:

$$d_i = D \left[\frac{\rho_f(\rho_i - \rho_f)g}{\mu^2} \right] \quad (2)$$

$\theta_{cr,i}$ = Shields parameter

D = Diameter of sediment types

ρ_f = Fluid density

ρ_i = Sediment density

g = Magnitude of the acceleration of gravity

μ = Dynamic viscosity of the fluid

b. Background transport equations

The following equations can be used to calculate bed sediment:

■ Meyer Peter Müller

This is the most commonly used equation for sediment transport. It is an empirical equation for calculating bed transport. The experiments to obtain this equation were carried out in sand and gravel channels, using natural and synthetic materials with a diameter range between 0.4 and 30 mm (Meyer-Peter & Müller, 1948):

The Meyer-Peter-Müller equation establishes the following hypotheses (Bravo, Osterkamp, & Lopes, 2004):

The capacity of the flow to transport sediment in the granular bed is directly related to the difference in hydraulic stress on the sediment particles and the critical shear stress at the start of movement.

- ◆ The energy loss depends on the resistance of sediment movement.
- ◆ Flow acting on the bed decreases the traction force of sediment transport.
- ◆ Different particle sizes are represented by the mean diameter.
- ◆ Unconsolidated sediment transport occurs on the bed, generating dunes and other forms.
- ◆ Bottom sediment transport is generated in particles with diameters greater than 0.4 mm.

- Nielsen

Semi-empirical equation for calculating bed transport (Nielsen, 1992). The experiments to obtain this equation were conducted using fine sediment, which was finer than that used in the derivation of the Meyer-Peter-Müller equation (Higgins et al., 2017)

- Van Rijn

Empirical equation based on sediment transport experiments carried out with granular material in a size range of 0.2 to 2 mm. According to the parameters involved in the equation, bed movement in the bed begins when the effective force of the fluid exceeds the resistance of the particles to be moved (weight and friction), establishing a final condition based on the angle of repose of the particles (Rijn, 1984). In the case where the material is composed of a significant percentage of clays or silts, it is necessary to consider the effects of cohesion (Rijn, 1993).

The Meyer-Peter-Müller equation was selected for the calculation of bed sediment transport, since the sediment diameters used in the physical and numerical model are within the recommended range for the use of the equation. The equation is as follows (Meyer-Peter & Müller, 1948):

$$q_{b,i} = \Phi_i \left[g \left(\frac{\rho_i - \rho_f}{\rho_f} \right) D^3 \right]^{\frac{1}{2}} \quad (3)$$

Where:

$q_{b,i}$ = Volumetric transport fraction of bed drag

Φ_i = Dimensionless fraction of bed load transport

$$\Phi_i = \beta_{\text{MPM},i} (\theta_i - \theta_{\text{cr},i})^{1.5} c_{b,i} \quad (4)$$

D = Diameter of sediment types

ρ_f = Fluid density

ρ_i = Sediment density

g = Magnitude of the acceleration of gravity

$\beta_{\text{MPM},i}$ = coefficients equal to 8.0 $c_{b,i}$

θ_i = Local shields parameter

$$\theta_i = \frac{\tau}{g * D (\rho_i - \rho_f)} \quad (5)$$

τ = Bed shear stress

$c_{b,i}$ = Volume fraction of material i in the bed

c. Richardson-Zaki multiplier coefficient, suspended sediment diffusion and turbulent diffusion multiplier

The Richardson-Zaki multiplier coefficient is a coefficient that controls the effect of drag on sediment particles that settle as they concentrate. The default value is 1.0.

Suspended sediment diffusion is considered if the molecular diffusion coefficient or turbulent diffusion is defined with a value other than zero.

The turbulent diffusion multiplier is the inverse of the Schmidt number, usually defined around 1.43 (FLOW-3D, n.d.).

The default values have been taken by the software since there is no specific analysis in the physical model related to the coefficients in question.

d. Maximum compaction fraction

This value controls the maximum solid fraction when the sediment is compacted. The default value is 0.64, which corresponds to the maximum sphere compaction fraction. For multi-dispersed sediments, this number can be higher for irregular and mono-dispersed sediment particles (Jurado & Oñate, 2020).

e. Bed roughness / D_{50} ratio

The d_{50} is the sediment size such that 50% of the weight of the material is smaller than it, and it is calculated for each time step and for each mesh cell with sediment. The recommended value for the multiplier of this ratio is 2.5 (FLOW-3D, n.d.), and this value has been adopted in the model.

f. Sediment types

The maximum number of sediment types that can be defined in the software is 10 (FLOW-3D, n.d.), and the sediment particle size of the physical model was placed in the numerical model. For the numerical model, the three sediment sizes with the highest percentage of weight retained were selected, corresponding to the sediment of 0.85, 0.71 and 0.6 mm, with 20.4, 36.7 and 36.6% respectively. The weights are entered without decimals and the program automatically calculates the percentages. For each type of sediment, it is optional to enter the name; if a name is not provided, the default name is "Sediment #", in this case the sieve number has been entered. The diameter of each type of sediment is the average particle size in meters. The particle density must be specified by the user, since no default value is used. The value of the particle density in the physical model is 2650 kg/m³ (Gallardo, 2019).

The critical Shields number is calculated using the Soulsby-Whitehouse equation (Soulsby, 1997). The critical Shields number can be modified on a cell-by-cell basis at each time step, to account for the effect of bed slope. At a sloping bed interface, gravity applies a tangential component of force to make the sediment bed more or less stable depending on the flow direction. In this case, the bed slope is close to horizontal so such consideration is not necessary.

The drag coefficient controls the rate at which sediment is eroded at a given shear stress greater than the critical shear stress. It can be used to scale transport rates or fit experimental data. The default value is 0.018 (Mastbergen & Van Den Berg, 2003). A value of zero disables the drag model completely. The default value has been set.

The bed load coefficient controls the rate at which bed load transport occurs at a given shear stress greater than the critical shear stress. The value depends on the bed transport equation selected. A value of zero turns off the sediment transport model. For the Meyer-Peter and Mueller equation, researchers have suggested values ranging from 5.0 for low transport to 13.0 for very high sand transport (Fernández & Van Beek, 1976). The value of 13.0 has been selected since sand transport is at high values according to the physical model (Chiliquinga & Pinto, 2019).

The angle of repose describes the maximum angle of repose of the bed material. For sand, values between 25 and 35 degrees are recommended, and for gravel, between 30 and 40 degrees, since the bed material is sand and an angle of repose value of 25 degrees has been set.

Turbulence and viscosity: Sediment transport requires accurate estimates of shear stresses, so a turbulence model for turbulent flows must be selected (FLOW-3D, n.d.). The viscous fluid option was selected and the two-equation k-w turbulence model was adopted, since this turbulence model was recommended in the project: "Analysis of Sediment Transport Downstream of Submerged Panels Applying the Flow 3D Program" after the comparison of results and

sensitivity analysis between the k-E, k-w and RNG models (Jurado and Oñate, 2020). The parameters were analyzed: model solution time, Reynolds number, velocities between the physical and experimental model, reaching the conclusion that the k-w turbulence model is the one that best fits the physical model (Jurado & Oñate, 2020).

Density variation: by default, the variable density model will be activated to allow the fluid density to be calculated based on the entrained suspended sediment (FLOW-3D, n.d.).

2.2.3 Fluid selection

The fluid selected was water at a temperature of 20°C, with a density of 1000 kg/m³ and a constant viscosity.

2.2.4 Meshing

To place an appropriate mesh, a sensitivity analysis was performed, and the results are presented in the following table:

Table 2. Summary of the mesh sensitivity analysis

Square pile	General mesh (m)	Pile mesh (m)	Simulation time (hh:mm:ss)	Remarks
Analysis 1	0.01	0.01	-	Model not convergent.
Analysis 2	0.05	0.05	15:02:59	Full meshing of the geometry. The model was not calibrated.
Analysis 3	0.05	0.01	40:00:00	Full meshing of geometry. Simulation not completed.
Analysis 4	0.05	0.01	15:16:23	Optimized meshing, from the center of the stack 30 cm on the X and Y axis on each side. Calibration achieved.

The sensitivity analysis aims to understand the behavior of the model and its response to changes induced in physical and numerical parameters. In this case, the model was optimized to obtain the limiting mesh size whose results fit the calibration by optimizing simulation times. It was concluded that the optimal mesh is a hexahedral structured mesh of 0.05 × 0.05 m in general and 0.01 × 0.01 m in the pile. The mesh was optimized to achieve a shorter run time with adequate results. The numerical model approximated the physical one, achieving an error between 0.0 and 10.0% at different times. The mesh was placed from the center of the pile 30 cm on the X and Y axis on each side and for the piles the mesh was placed 10 cm on each side. On the Z axis, the mesh was placed from the bottom of the channel to 28 cm above the sand bed.

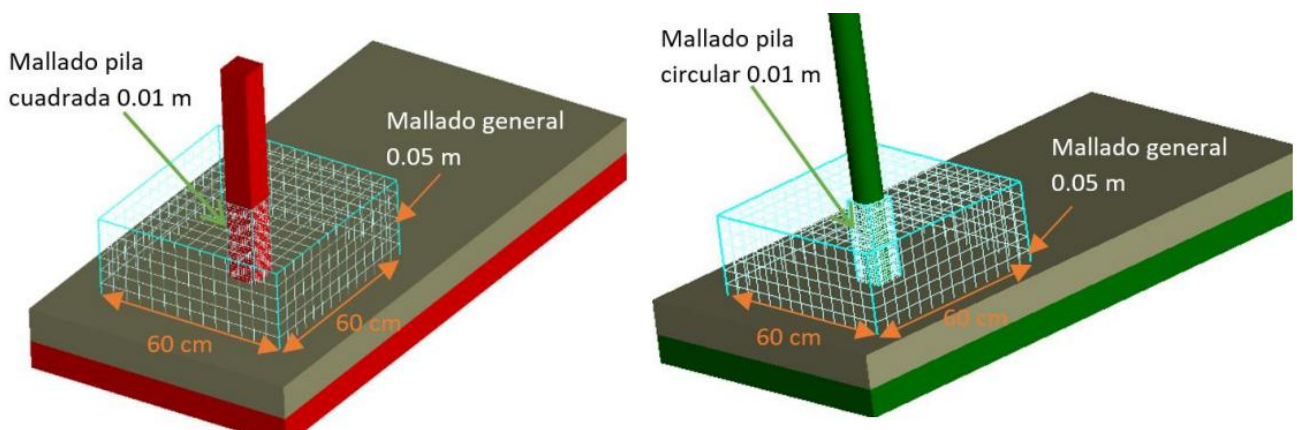


Figure 3. Meshing for the square and circular stack.

2.2.4 Boundary conditions

The boundary conditions for the numerical model are entered based on the analysis conditions established in the physical model.

X minimum. - Inlet flow rate (Q) was set, with a constant flow rate of 52.47 l/s, depth of 25 cm above the surface of the sand bed.

X maximum. - Pressure (P) was set, with a fluid elevation of 25 cm (condition that specifies the pressure at the outlet boundary by means of the fluid elevation).

Y minimum, Y maximum and Z minimum. - Symmetry (S) was set, so that the mesh boundaries and the base of the channel do not interfere with the results of the run.

Z maximum. - Pressure (P) was set, with zero fluid elevation to indicate that at the Z maximum boundary the manometric pressure is zero.

A depth of 25 cm above the sand bed was set as an initial condition to avoid sediment disturbances during the flow inflow.

2.2.5 Simulation time

The simulation time is the period during which the phenomenon occurs and defines the end of the simulation. The numerical model was run for 4 hours, which corresponds to the analysis time of the physical model. An interval of one second was entered for the output of results.

3. Results

3.1 Calibration

To calibrate the physical model, the results of maximum erosion around the pile of the numerical model and the physical model at different times were compared. The values obtained are presented in the following table:

3.1.1 Calibration results for the square pile

Table 3. Calibration results for the square stack

Time (hours)	Maximum erosion (cm)		Difference (%)
	Physical model	Numerical model	
0	0	0	0.00%
1	5	5.5	10.00%
2	10	10.25	2.50%
3	12	11.83	1.42%
4	12	12	0.00%

The numerical model of the square pile was calibrated with a maximum percentage of 10% difference between the maximum erosion results between the physical and numerical model. Figure 4 shows the level of the sand bed in 4 hours of modeling on axes placed in the X and Y direction in the area of maximum erosion around the pile.

Figure 5 shows the similarity of maximum erosion around the square pile in the physical and numerical model, and the elevation of the bed has a minimum value of 0.10 m around the pile, this value represents the elevation of the base of the channel, therefore, the maximum erosion is 12 cm.

3.1.2 Calibration results for the circular pile

In the numerical calibration model, it was evident that the mesh used in the area of the circular pile does not fit properly to the general mesh, due to its shape; several meshing attempts were made to achieve a correct geometric

interpretation in the mathematical space without achieving convergence of the model. The computational package generates results in the general meshing that are not related to the results of the meshing around the pile; for this reason, it was not possible to make the comparison between the physical model and the mathematical model for calibration. The separation of the meshes can be seen in the following figure.

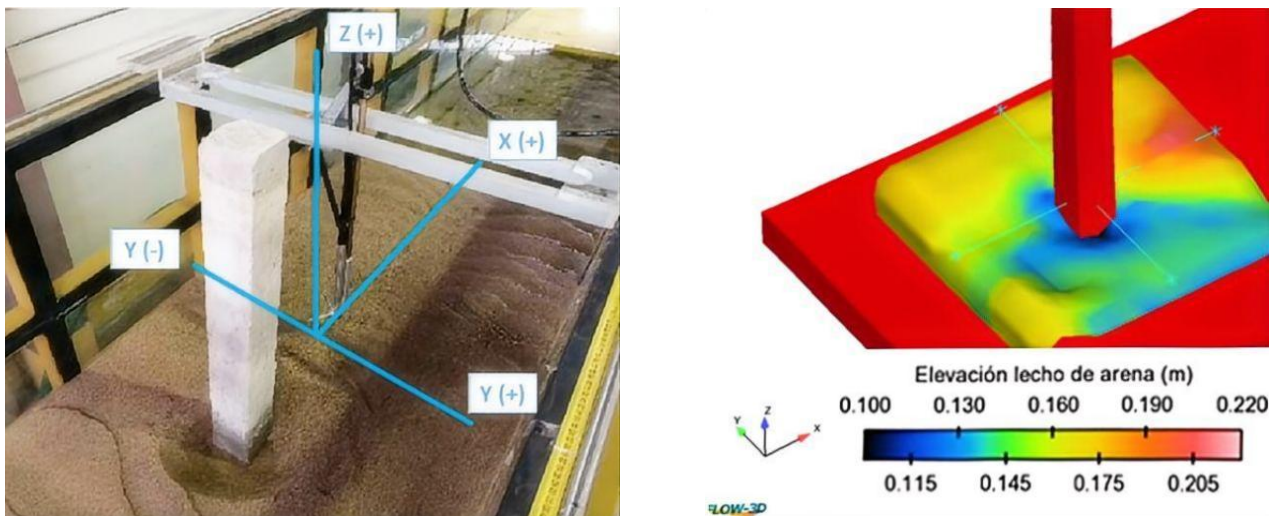


Figure 4. Calibration of the square pile numerical model.

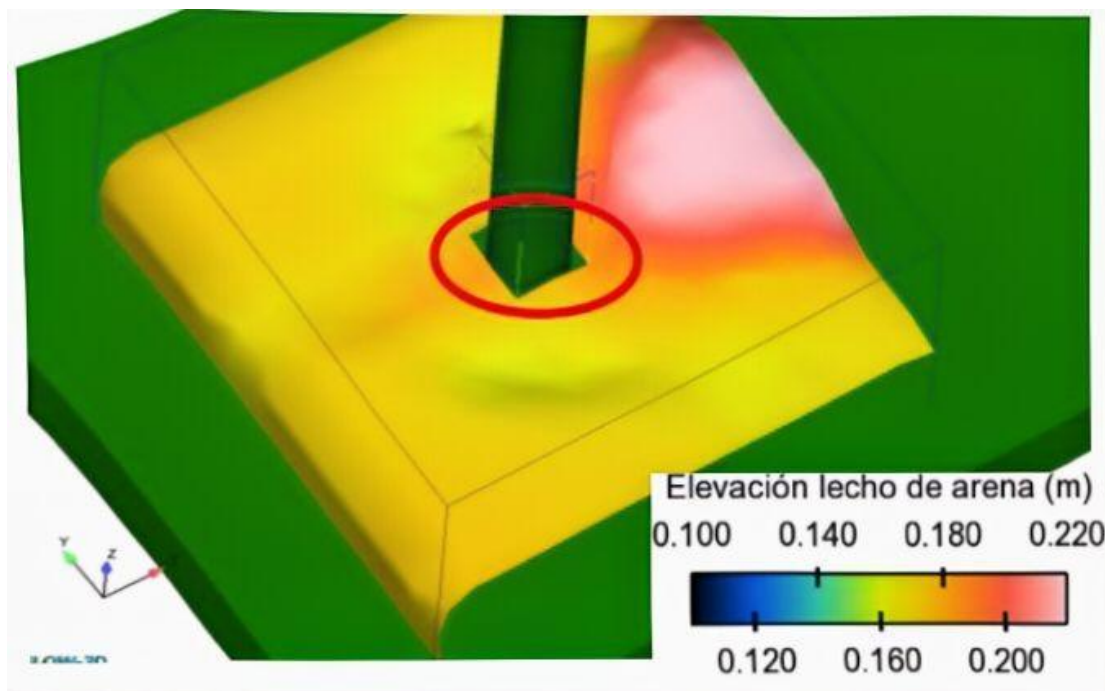


Figure 5. Circular stack numerical model.

3.2 Improved model (square pile)

Since it was not possible to determine the maximum erosion around the pile in the physical model because the sediment bed was 12 cm high, a 20 cm high bed was placed in the improved numerical model, maintaining the same geometric, physical and contour characteristics of the calibrated model. To evaluate the maximum erosion around the square pile, the run time was increased to 8 hours. The results of the improved model are presented below:

Table 4. Maximum erosion results around the square pile

Time (hours)	Maximum erosion (cm)
0	0
1	4.7
2	9.8
3	12
4	14.4
5	14.6
6	14.7
7	14.8
8	15

After 8 hours, the numerical model stabilizes and reaches a maximum erosion of 15 cm. In the project in which the physical model was carried out (Chiliquinga & Pinto, 2019), the maximum erosion was estimated by using empirical equations from various authors. Below is a comparison of the results of the improved model and the estimate of the maximum erosion:

Table 5. Results of maximum erosion around the square pile

Item	Maximum erosion (cm)	Difference (%)
Physical model	15	-
Laursen and Toch equation	20	25.00%
Maza-Sanchez equation	18	16.67%
Melville and Coleman equation	21.12	28.98%
CSU equation	13.87	8.15%
Froehlich equation	16.35	8.26%

Source: Chiliquinga and Pinto (2019)

The result of maximum erosion around the square pier in the physical model is close to the values calculated with the CSU and Froehlich equations with similarity percentages of 91.85% and 91.74% respectively.

4. Conclusions

- For the numerical modeling of the analysis of erosion around bridge piers, the FLOW-3D computational package was used. This software allows the calculation of sediment movement by predicting erosion, advection and sedimentation.
- The FLOW-3D model is limited to the use of computers with high processing and storage capacity, so a work station with an Intel Xeon processor with a base speed of 2.2 GHz was used. This processor has 12 cores and 24 logical processors, 64 Gb installed RAM and a 4Gb graphics processor.
- To determine the optimal mesh, a sensitivity analysis was performed with different mesh sizes, obtaining as a result a general mesh of 0.05×0.05 m and a pile mesh of 0.01×0.01 m so that the program can properly interpret the geometry of the pile.
- The numerical model of the square pile was calibrated by comparing the maximum erosion around the pile between the physical and numerical models, obtaining a maximum difference of 10% in one hour and 0% in four hours.

- The numerical model of the circular pile was not calibrated, because the general mesh and the pile mesh do not fit properly. It is recommended to use software that allows unstructured meshing so that the geometric interpretation adapts to the circular shape.
- The numerical model of the square pile stabilizes after 8 hours of simulation, with a result of maximum erosion around the pile of 15 cm. When comparing the result with the calculation of maximum erosion estimates using several proposed empirical equations, it is evident that the result fits 91.85% with the result of the CSU equation and 91.74% with the result of the Froehlich equation.
- By adequately representing a numerical model of the erosion phenomenon around bridge piers, it is also possible to simulate solutions, for example, the use of submerged panels placed individually, in series or in parallel, with different angles of attack towards the pier. These results would allow solving bridge failures due to scour related to hydraulic problems. For this reason, with the results of this research, we have the basis to continue with the investigation of the proposed solutions.

Conflicts of Interest

The author declares no conflicts of interest regarding the publication of this paper.

References

- [1] Bravo, M., Osterkamp, P., & Lopes, L. (2004). Transporte de sedimentos en corrientes naturales. *Terra Latinoamericana*, 22(3), 377-386. <https://www.redalyc.org/pdf/573/57322315.pdf>
- [2] Chilinginga, J., & Pinto, C. (2019). Análisis experimental en modelo físico de fenómenos de turbulencia causantes de erosión alrededor de pilas de puentes utilizando acoustic doppler velocimeter ADV [Tesis de pregrado, Escuela Politécnica Nacional]. Repositorio digital institucional de la Escuela Politécnica Nacional. <https://bibdigital.epn.edu.ec/handle/15000/20363>
- [3] Chow, V. (2004). *Hidráulica de canales abiertos*. Nomos S.A.
- [4] Fernández Luque, R., & Van Beek, R. (1976). Erosion and transport of bed-load sediment. *Journal of Hydraulic Research*, 14(2), 127 - 144. <https://doi.org/10.1080/00221687609499677>
- [5] Fernández, M. (2004). Estudio de la evolución temporal de la Erosión Local en. Barcelona [Tesina]: UPCCommons. <https://upcommons.upc.edu/handle/2099.1/3343>
- [6] FLOW- 3D. (s.f.). Flow 3D Hydro user manual. Obtenido de <https://C:/flow3d/HYDROv1.0u1/help/index.html>
- [7] Gallardo, K. (2019). Demostración experimental del efecto de los paneles sumergidos en la erosión local de pilas de puentes cuadradas. Quito, Pichincha, Ecuador [Tesis de pregrado, Escuela Politécnica Nacional]. Repositorio digital institucional de la Escuela Politécnica Nacional. <https://bibdigital.epn.edu.ec/handle/15000/20172?locale=de>
- [8] Hamad, K. (2015). Submerged Vanes Turbulence Experimental Analysis [Tesis doctoral, Universitat Politècnica de Catalunya]. TDX. <http://hdl.handle.net/10803/377436>
- [9] Higgins, A., Restrepo, J., Otero, L., Ortiz, J., & Conde, M. (2017). Distribución vertical de sedimentos en suspensión en la zona de desembocadura. *Latin american journal of aquatic research*, 45(4), 724-736. <http://dx.doi.org/10.3856/vol45-issue4-fulltext-9>
- [10] Jurado, L., & Oñate, V. (Julio de 2020). Análisis del transporte de sedimentos aguas abajo de paneles sumergidos aplican. Quito, Ecuador [Tesis de postgrado, Escuela Politécnica Nacional]. Repositorio digital institucional de la Escuela Politécnica Nacional. <https://bibdigital.epn.edu.ec/handle/15000/20172?locale=de>
- [11] Mastbergen, D., & Van Den Berg, J. (2003). Breaching in fine sands and the generation of sustained turbidity currents in submarine canyons. *Sedimentology*, 50(4), 625 - 637. <https://doi.org/10.1046/j.1365-3091.2003.00554.x>

[12] Meyer-Peter, E., y Müller, R. (1948). Formulas for Bed-Load Transport. Proceedings of the 2nd Meeting the International Association for Hydraulic Structures Research, Delft, 39-64. <http://resolver.tudelft.nl/uuid:4fda9b61-be28-4703-ab06-43cdc2a21bd7>

[13] Nielsen, P. (1992) Coastal Bottom Boundary Layers and Sediment Transport. World Scientific. <https://doi.org/10.1142/1269>

[14] Rijn, Van. (1984). Sediment transport, Part I: bed load transport. Journal of Hydraulic, 110(10). 1613-1641. [https://doi.org/10.1061/\(ASCE\)0733-9429\(1984\)110:10\(1431\)](https://doi.org/10.1061/(ASCE)0733-9429(1984)110:10(1431))

[15] Rijn, Van. (1993). Principles of sediment transport in rivers, estuaries and coastal seas. Aqua, Amsterdam Publications.

[16] Shields, A. (1936). Application of similarity principles and turbulence research to bed-load movement. Mitteilungen der Preußischen Versuchsanstalt für Wasserbau. <http://resolver.tudelft.nl/uuid:a66ea380-ffa3-449b-b59f-38a35b2c6658>

[17] Soulsby, C. (1997). Bed load transport. In Dynamics of Marine Sand. Thomas Telford Publications.

[18] Weig, G, Brethour, J., Grunzner, M., y Burnham, J. (2014). The sediment Scour Model in Flow 3D. Flow Science.